IMMUNOLOGY

CD1d1 intrinsic signaling in macrophages controls NLRP3 inflammasome expression during inflammation

Shan Cui[1]*, Chenhui Wang[2]*, Weizhi Bai[3]*, Jiao Li[4], Yue Pan[2], Xiaoyong Huang[2], Han Yang[2], Zeqing Feng[2], Qun Xiang[2], Lei Fei[2], Lixin Zheng[5], Jian Huang[3]†, Qinggao Zhang[4]†, Yuzhang Wu[2]†, Yongwen Chen[2]†

Dysregulation of immune responses in the gut often associates with inflammatory bowel diseases (IBD). Mouse CD1d1, an ortholog of human CD1d mainly participating in lipid-antigen presentation to NKT cells, is able to generate intrinsic signals upon stimulation. Mice with macrophage-specific *CD1d1* deficiency (*Lym*$^{CD1d1-/-}$) acquire resistance to dextran sodium sulfate (DSS)–induced colitis, attributing to the transcriptional inhibition of NLRP3 inflammasome components. The hyperactivation of NLRP3 inflammasome accounts for gut epithelial proliferation and intestine-blood barrier integrity. Mechanistically, occupancy by the natural ligand glycosphingolipid iGb3, CD1d1 responds with intracellular Ser^{330} dephosphorylation thus to reduce the Peroxiredoxin 1 (PRDX1)–associated AKT-STAT1 phosphorylation and subsequent NF-κB activation, eventually causing transcriptional down-regulation of *Nlrp3* and its immediate substrates *Il1b* and *Il18* in macrophages. Therefore, the counterbalancing role of CD1d1 in macrophages appears to determine severity of DSS-mediated colitis in mice. These findings propose new intervention strategies for treating IBD and other inflammatory disorders.

INTRODUCTION

Ulcerative colitis and Crohn's disease are the most common forms of human inflammatory bowel disease (IBD). Although the definitive etiology remains unknown, development of IBD is widely considered as the result of misinteraction of genetic and environmental factors that triggers autoimmune responses in the host (*1*). Experimental colitis models have been established by oral administration of dextran sodium sulfate (DSS) in animals for induction of human IBD-like clinical syndromes that manifest with mucin depletion, epithelial degeneration, apoptosis, and dysregulation of gut microbiota (*2*). DSS-induced acute colitis in mice has been effective in exploring pathogenesis and therapeutics of human IBD.

Mouse CD1d1 belongs to the CD1d superfamily protein by sharing structural and functional homologies to the major histocompatibility complex (MHC) molecules. CD1d1 specifically activates a population of unconventional T cells named natural killer T (NKT) cells through presenting antigenic self-lipids or certain glycolipids derived from pathogenic bacteria, commensals, and fungi (*3*). CD1d1 also transmits reciprocal signals to trigger cytokine production from CD1d1-expressing intestinal epithelial cells (IECs) and monocytes (*4*). Functional studies of CD1d1 in the pathogenesis of DSS-mediated colitis have generated controversial results, with one work indicating that *CD1d1*$^{-/-}$ mice have no difference in development of DSS-colitis (*5*) versus other reports claiming that *CD1d1*$^{-/-}$ mice are more sensitive to DSS-induced colitis (*6*, *7*). Moreover, a recent work has mentioned that *CD1d1* in the epithelium elicits protective effects on acute colitis by promoting interleukin-10 (IL-10) production (*8*). Although the basis for this discrepancy is unclear, it seems that CD1d1 expression on different cell types might bring forward diverse biological functions in controlling the progress of acute colitis.

NLRP3 (NLR family pyrin domain containing 3) inflammasome is a multiprotein complex comprising NLRP3, caspase-1, and the adaptor molecule ASC [apoptosis-associated peck-like protein with CARD (caspase recruitment domain) domain, Pycard]. Once activated, the inflammasome triggers proteolytic cleavage of dormant procaspase-1 into active caspase-1 by thus catalyzing conversion of precursors proIL-1β and proIL-18 into active IL-1β and IL-18, respectively (*9*). Normal activation of NLRP3 inflammasome appears to promote homeostatic restoration following traumatic tissue injuries; however, its dysregulation often associates with the exacerbation of inflammatory diseases including IBD (*10*). For example, single-nucleotide polymorphisms in NLRP3 gene are associated with susceptibility to ulcerative colitis (*11*). The roles of NLRP3 inflammasome in the pathogenesis of DSS-caused colitis have also been extensively studied, with the results showing that loss of epithelial integrity and massive leukocyte infiltration appear to associate with *Nlrp3*$^{-/-}$ and *Casp-1*$^{-/-}$ mice for developing more severe colitis (*12*). Our recent work has also demonstrated that dysregulation of NLRP3 inflammasome activity in *Vsig4*$^{-/-}$ [V-set and immunoglobulin (Ig) domain-containing 4] in mice renders protection to DSS-mediated colitis (*13*). However, factors that induce NLRP3 inflammasome hyperactivation within colonic tissues in response to DSS are still unclear.

We here show that mice with *CD1d1* deficiency or specific deletion of *CD1d1* in macrophages (*Lym*$^{CD1d1-/-}$) are resistant to DSS-induced acute colitis. This protective effect attributes to the increase in colonic biosynthesis of NLRP3 and the inflammasome substrates IL-1β and IL-18. Further studies demonstrate that iGb3 occupancy of CD1d1 initiates the intracellular domain Ser^{330} dephosphorylation, which results in a reduction of signaling through the AKT–signal transducers and activators of transcription 1

[1]Yanbian University Hospital, Yanbian University, Jilin Province 133000, People's Republic of China. [2]Institute of Immunology, PLA, Third Military Medical University, Chongqing 400038, People's Republic of China. [3]Department of Emergency, Chongqing University Center Hospital, Chongqing Emergency Medical Center, Chongqing 400038, People's Republic of China. [4]School of Medicine, Yanbian University, Jilin Province 133000, People's Republic of China. [5]Laboratory of Immune System Biology, National Institute of Allergy and Infectious Diseases, NIH, Bethesda, MD, USA.
*These authors contributed equally to this work.
†Corresponding author. Email: chenyongwen@tmmu.edu.cn (Y.C.); wuyuzhang@tmmu.edu.cn (Y.W.); zqg0621@ybu.edu.cn (Q.Z.); 85408306@qq.com (J.H.)

(STAT1)–Peroxiredoxin 1 (PRDX1)–nuclear factor κB (NF-κB) cascades, eventually down-regulating *Nlrp3*, *Il1b*, and *Il18* gene expressions in macrophages.

RESULTS

CD1d1$^{-/-}$ mice acquire protection from DSS-induced mortality and morbidity

To investigate the role of CD1d1 in disease progression after gut mucosal injury, 8-week-old male mice were continuously given 3.0% DSS in drinking water for 6 days to induce acute colitis. The survival rate of *CD1d1*$^{-/-}$ mice was significantly higher than *WT* littermates (Fig. 1A). DSS-treated *CD1d1*$^{-/-}$ mice exhibited considerably less body weight loss, lower disease activity indices (Fig. 1B), and longer colon length presentation as compared to *WT* controls (Fig. 1C). Intestine-blood barrier tests by orally administering fluorescein isothiocyanate (FITC)–dextran showed that the diffusion of FITC-dextran across the epithelium was significantly lower in *CD1d1*$^{-/-}$ mice (Fig. 1D). Hematoxylin and eosin (H&E) staining showed that colonic tissues from *WT* mice were more severe in immune cell infiltration, epithelial injury, crypt hyperplasia, and edema than *CD1d1*$^{-/-}$ animals (Fig. 1E). These data suggest that *CD1d* deficiency renders mice a marked resistance to DSS-mediated colitis.

Dysregulation of the NLRP3 inflammasome has been shown to affect the pathogenesis of DSS-induced acute colitis (*12*, *13*). Therefore, we investigated the functions of CD1d1 in the activation of DSS-induced NLRP3 inflammasome. Comparing with *WT* controls, the colonic homogenates from *CD1d1*$^{-/-}$ mice exhibited with elevation of NLRP3, along with increasing of the activated forms of caspase-1, IL-1β, and IL-18 (Fig. 1F). In light of IL-1β as capable of promoting production of IL-22 and IL-10 and both of these cytokines appear to maintain colonic epithelial integrity (*14*, *15*), we observed slight increases in IL-10 and IL-22 expression in DSS-treated *CD1d1*$^{-/-}$ colonic homogenates (Fig. 1F). IL-18 and IL-1β have been suggested to be protective against DSS-induced inflammatory colonic damage through inducing a compensatory epithelial proliferative response (*12*). In agreement, we found that the colonic tissues from DSS-treated *CD1d1*$^{-/-}$ mice expressed high levels of proliferating cell nuclear antigen (PCNA) (Fig. 1, F and G). The DSS-treated *CD1d1*$^{-/-}$ mice also showed a better preservation of the integrity of gut epithelial barrier as evidenced by decreased infiltration of proinflammatory CD45$^+$ leukocytes, CD45$^+$ly6G^{high} neutrophils, and CD45$^+$F4/80$^+$ macrophages in the affected colon tissues (Fig. 1H). The hyperactivation of NLRP3 inflammasome and overburden of IL-1β can promote the differentiation of CD4$^+$Foxp3$^+$ T regulatory cells (T_{regs}), which play an essential role in maintaining homeostasis and combating inflammatory conditions in the gut. Flow cytometry showed that the colonic tissues from *CD1d1*$^{-/-}$ mice have a significantly higher percentage of T_{regs} than *WT* littermates after DSS administration (Fig. 1H).

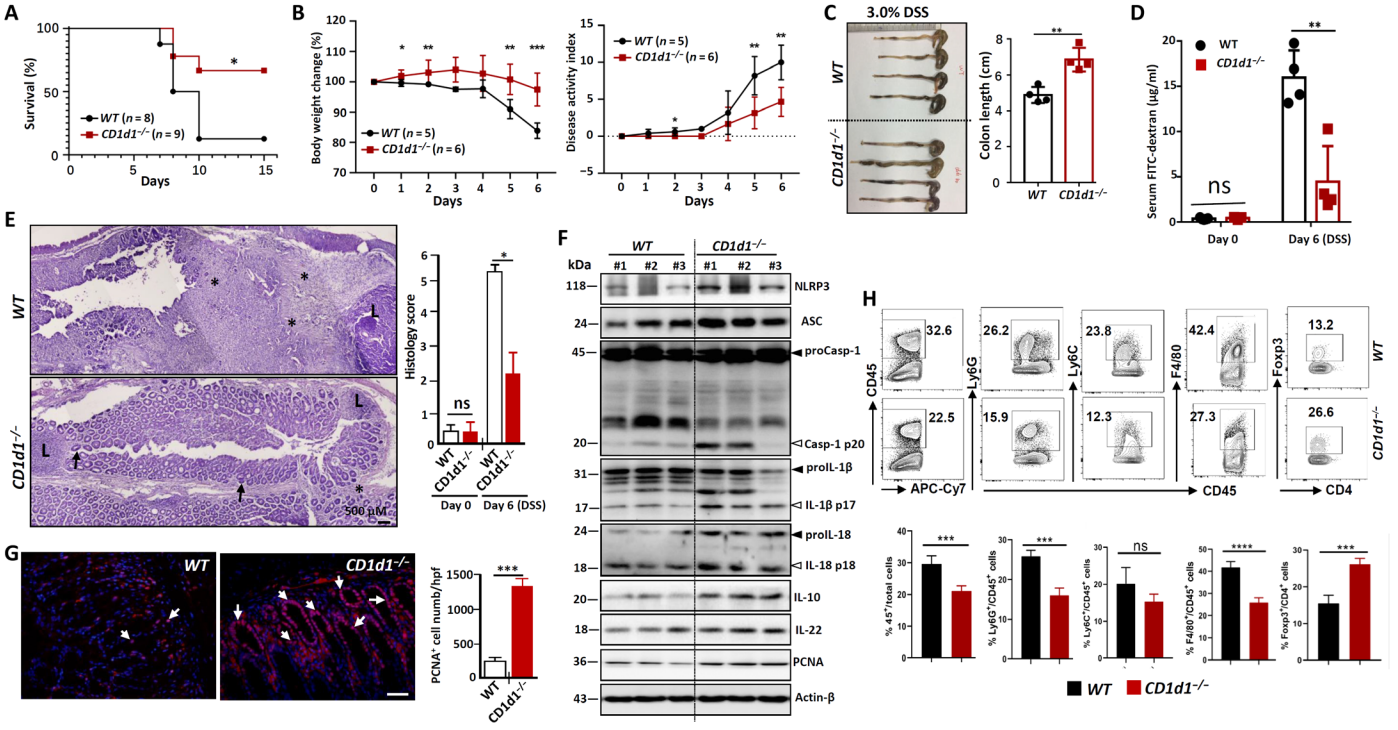

Fig. 1. *CD1d1* deficiency protects mice from DSS-induced colitis. Eight-week-old male mice were given 3.0% DSS in drinking water for six continuous days. Comparative analyses of (**A**) the survival rate and (**B**) body weight loss and disease activity index. On day 6, mice were euthanized, and the colonic tissues were collected. (**C**) Measurement of colon length, (**D**) serum permeability tracer FITC-dextran, and (**E**) H&E staining analysis of histopathological changes (left) and semi-quantitative scoring of histopathology (right). Asterisks indicate severe edema/inflammation with large lymphoid nodules (L), and arrows indicate retention/regeneration of crypt, $n = 6$ to 8 per group; (**F**) immunoblotted for the indicated proteins; (**G**) in situ immunofluorescence analysis of PCNA expression, arrows indicate positive cells, and blue indicates DAPI. Scale bar, 30 μm. (**H**) Representative flow cytometry plots for the indicated cells infiltrated (top) and the percentage of the indicated cells within colonic tissues were compared (bottom). Error bar, SEM. *$P < 0.05$, **$P < 0.01$, ***$P < 0.001$, and ***$P < 0.0001$. ns, no significant difference. Data in (A) were analyzed by the log-rank test, and others were compared by Student's *t* test; one of four representative experiments with similar results was shown. hpf, high-power field.

The unexpected protective phenotype of *CD1d1* deficiency led us to examine NLRP3 inflammasome functions. We found that *Nlrp3*$^{-/-}$ mice manifested with considerably more body weight loss, more severe disease indices, and significantly lower survival rates as compared to *WT* controls (fig. S1). We also generated *CD1d1*$^{-/-}$*Nlrp3*$^{-/-}$ double knockout (DKO) mice and found that these mice developed more deteriorated colitis compared to *WT* and *CD1d1*$^{-/-}$ mice following 3.0% DSS administration (fig. S1). These data suggest that *CD1d1*$^{-/-}$ mice are protected against DSS-caused colitis through inducing NLRP3 inflammasome hyperactivation.

CD1d1 expression in hematopoietic cells determines the severity of DSS-colitis in mice

To address what type of cells are responsible in mediating the CD1d1-dependent hypersusceptibility to DSS colitis, we generated four groups of CD1d1 bone marrow chimeras and subjected these mice to DSS-induced colitis. Concurring to observations in the conventional *CD1d1*$^{-/-}$ mice (Fig. 1), the *CD1d1*$^{-/-}$ autotransplantation group (*CD1d1*$^{-/-}$>*CD1d1*$^{-/-}$) presented with significantly milder signs of DSS colitis relative to *WT* autotransplantation group (*WT*>*WT*) (Fig. 2, A and B). However, *CD1d1*$^{-/-}$ mice that received *WT* bone marrow (*WT*>*CD1d1*$^{-/-}$) manifested with more severe colitis (Fig. 2, A and B), along with deteriorated colonic inflammatory histopathology (Fig. 2C) and shorter colon length presentation (Fig. 2D), as compared to *CD1d1*$^{-/-}$ autotransplantation group. Whereas the irradiated *WT* mice taking *CD1d1*$^{-/-}$ bone marrow (*CD1d1*$^{-/-}$>*WT*) appeared to gain resistance to DSS-induced colitis as compared to the *WT* autotransplantation group (Fig. 2, A to D).

In response to DSS stimulation, colon tissues from the *WT* bone marrow–transplanted *CD1d1*$^{-/-}$ recipient mice (*WT*>*CD1d1*$^{-/-}$) exhibited with reduced protein expression for NLRP3, Caspase-1p20, IL-1βp17, and IL-18 as compared to the *CD1d1*$^{-/-}$ autotransplantation group. Conversely, the colon homogenates from *WT* mice receiving *CD1d1*$^{-/-}$ bone marrow (*CD1d1*$^{-/-}$>*WT*) presented increasing protein expression for NLRP3, Caspase-1p20, IL-1βp17, and IL-18p22 (Fig. 2E). Overall, these combined data suggest that CD1d1-expressing hematopoietic cells rather than epithelial cells are accountable for sensitivity of the animals toward DSS-induced colitis through the control of NLRP3, IL-1β, and IL-18 expressions in vivo.

CD1d1 deficiency in macrophages protects mice from DSS-induced colitis

Flow cytometry showed that CD1d1 is constitutively expressed on the surface of many immune cells including monocytes, macrophages, neutrophils, dendritic cells (DCs), B cells, NK cells, and CD4$^+$ and CD8$^+$ T cells in circulation, with the highest detected on macrophages (Fig. 3A). Macrophages not only are important for maintaining the intestinal homeostasis but also provide an intracellular platform for assembly of NLRP3 inflammasome complex (*16*). Flow cytometry demonstrated that CD1d1 expresses on the surface of peritoneal macrophages (PEMs), bone marrow–derived macrophages

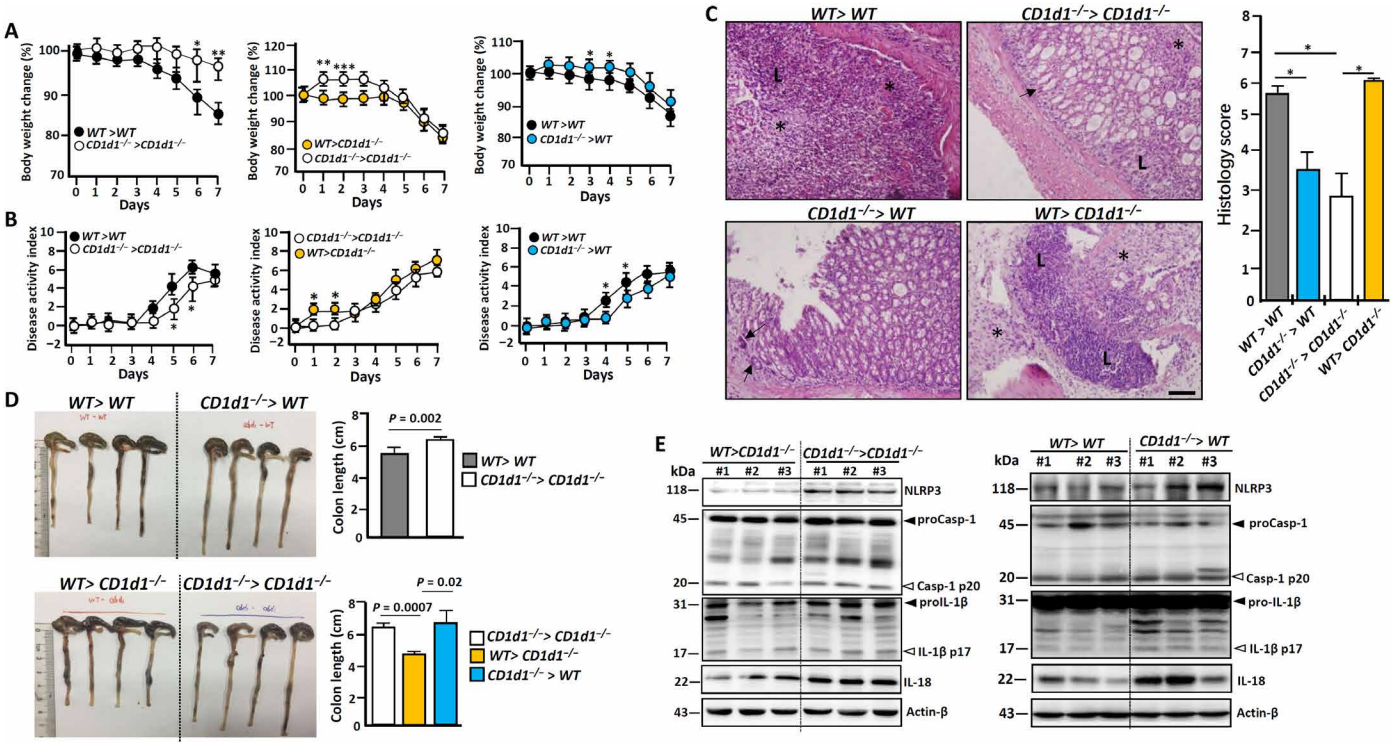

Fig. 2. Hematopoietic *CD1d1* deteriorates the severity of DSS-induced injury. Mice with bone marrow chimeras were given 3.0% DSS in drinking water for six continuous days. Comparative analyses of (**A**) body weight loss and (**B**) disease activity index. On day 6, mice were euthanized. (**C**) H&E staining analysis of histopathological changes (left) and semi-quantitative scoring of histopathology (right); asterisks indicate severe edema/inflammation with large lymphoid nodules (L), and arrows indicate retention/regeneration of crypt. Scale bar, 30 μm. (**D**) Measurement and analysis of colon length. (**E**) Colonic homogenates were immunoblotted for the indicated molecules. In (A) to (C), *WT*>*WT*, $n = 8$; *CD1d1*$^{-/-}$> *CD1d1*$^{-/-}$, $n = 14$; *WT*> *CD1d1*$^{-/-}$, $n = 7$; *CD1d1*$^{-/-}$>*WT*, $n = 9$. *$P < 0.05$, **$P < 0.01$, and ***$P < 0.001$ (Student's *t* test). Photo credit: Chenhui Wang, Institute of Immunology, PLA, People's Liberation Army of China; TMMU.

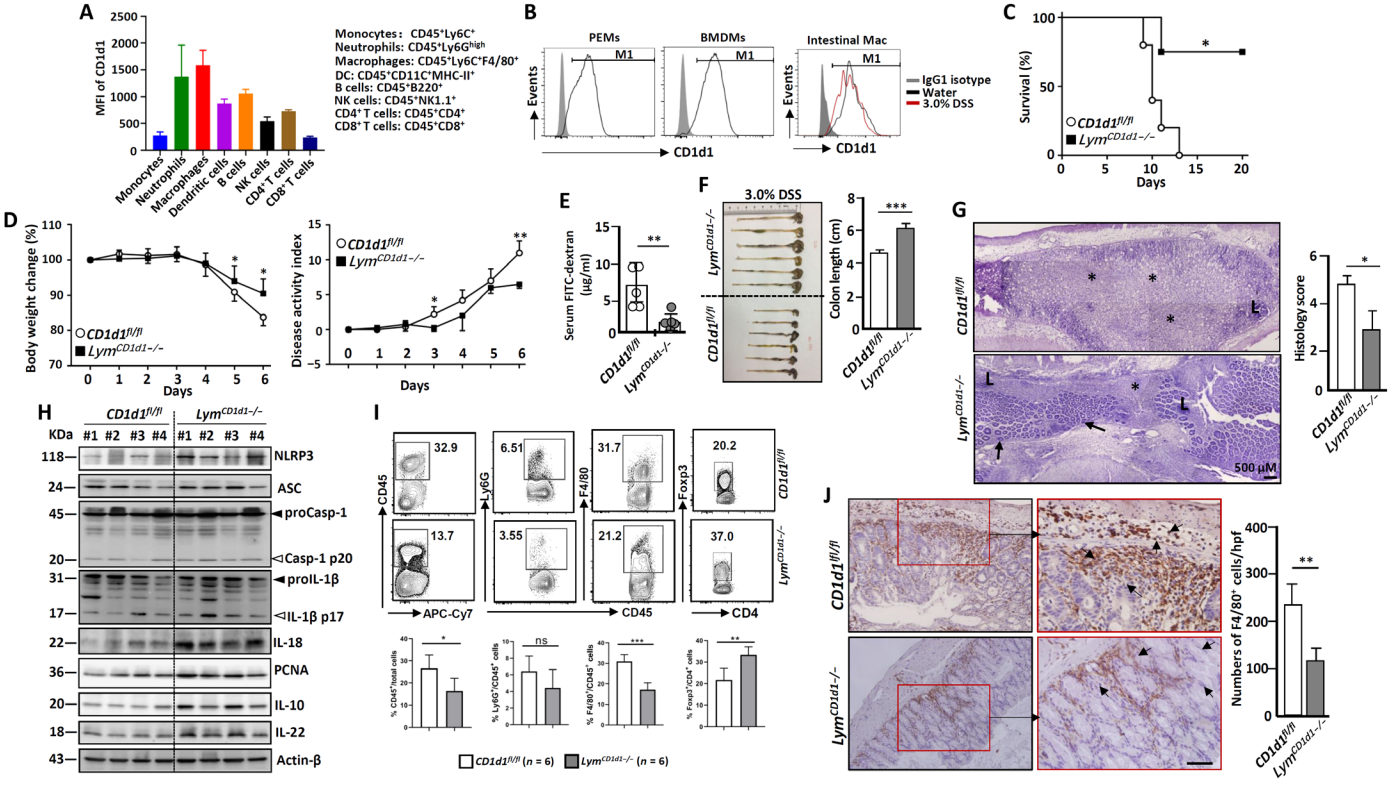

Fig. 3. *Lym*$^{CD1d1-/-}$ mice acquire protection from DSS-induced mortality and morbidity. Flow cytometry analysis of CD1d1 expression on surface of (**A**) indicated immune cells. (**B**) PEMs, BMDMs, and intestinal macrophages (Mac); gray lines indicate isotype controls. Eight-week-old male mice were continuously given 3.0% DSS in drinking water for 6 days. Comparative analysis of (**C**) the survival rate and (**D**) body weight loss and disease activity index. On day 6, mice were euthanized. (**E**) Serum permeability tracer FITC-dextran, (**F**) colon length, and (**G**) H&E staining analysis of colonic histopathological changes (left) and semi-quantitative scoring (right). Asterisks indicate severe edema/inflammation with large lymphoid nodules (L), and arrows indicate retention/regeneration of crypts. (**H**) Colonic homogenates were immunoblotted for the indicated proteins. (**I**) Representative flow cytometry plots for the indicated cells infiltrations (top) and percentage of indicated cells within colonic tissues (bottom). (**J**) Immunohistochemistry measurement of F4/80$^+$ macrophages in colonic tissues, and arrows indicate positive cells. Scale bar, 30 μm. Error bar, SEM. **P* < 0.05, ***P* < 0.01, and ****P* < 0.001. Data in (B) were analyzed by log-rank test, and others were compared by Student's *t* test. One of three representative experiments with similar results is shown. MFI, mean fluorescence intensity.

(BMDMs), and intestinal macrophages from mice with or without DSS administration (Fig. 3B). To examine the biofunction of macrophages-associated CD1d1, we generated mice with macrophage-specific *CD1d1* deletion (*CD1d1*$^{fl/fl}$ × *LyzM-cre*, hereafter referred to as *Lym*$^{CD1d1-/-}$). The resulting *Lym*$^{CD1d1-/-}$ mice are healthy and fertile, exhibiting no gross pathology. The *Lym*$^{CD1d1-/-}$ and *CD1d1*$^{fl/fl}$ male mice were subjected to 3.0% DSS-induced acute colitis. The survival rate of *Lym*$^{CD1d1-/-}$ mice was significantly higher than the *CD1d1*$^{fl/fl}$ littermates (Fig. 3C). DSS-treated *Lym*$^{CD1d1-/-}$ mice exhibited appreciably less body weight loss, lower disease indices (Fig. 3D), milder disruption of the intestine-blood barrier as indicated by lower levels of serum FITC-dextran concentrations (Fig. 3E), longer colon lengths (Fig. 3F), and less severe colonic damage (Fig. 3G) as compared to the *CD1d1*$^{fl/fl}$ control mice. In addition, colonic homogenates from DSS-treated *Lym*$^{CD1d1-/-}$ mice appeared to have elevated expressions of NLRP3, caspase-1p20, IL-1βp17, IL-18, PCNA, and the anti-inflammatory cytokines IL-10 and IL-22 (Fig. 3H). The DSS-treated *Lym*$^{CD1d1-/-}$ colon tissues presented with substantially less infiltration of CD45$^+$ leukocytes and pro-inflammatory F4/80$^+$CD45$^+$ macrophages while having markedly higher levels of Foxp3$^+$ T_{regs} (Fig. 3I). In situ immunohistochemistry also showed a reduction of infiltrating F4/80$^+$CD45$^+$ macrophages into *Lym*$^{CD1d1-/-}$ intestinal interstitial tissues (Fig. 3J). Collectively, these data demonstrated that *Lym*$^{CD1d1-/-}$ mice are resistant to DSS-induced colitis.

To address whether the dysregulation of the NLRP3 inflammasome is responsible for the protective phenotypes in *Lym*$^{CD1d1-/-}$ mice against DSS-mediated colitis, *Lym*$^{CD1d1-/-}$ mice were also given an intravenous injection with an IL-1 receptor antagonist (IL-1Rα; 2 μg per mouse per day) and IL-18 binding protein (IL-18BP; 200 ng per mouse per day) (*17*) for consecutive 5 days starting 1 day before 3.0% DSS treatment. As compared to the phosphate-buffered saline (PBS)–treated controls, blocking IL-1β and IL-18 signals in *Lym*$^{CD1d1-/-}$ mice resulted in significantly more body weight loss, higher colonic inflammatory necrosis, and severe disease scores (fig. S2), suggesting that the protection of *Lym*$^{CD1d1-/-}$ mice from DSS-mediated colitis relies on enhancing IL-1β and IL-18 production in vivo.

CD1d1 mediates transcriptional inhibition of *Nlrp3*, *Il1b*, and *Il18* in macrophages

We next examined whether CD1d1 can regulate NLRP3 inflammasome activation in macrophages in vitro. Quantitative reverse

transcription polymerase chain reaction (qRT-PCR) assessment of NLRP3 inflammasome component gene expression revealed that *CD1d1*-deficient BMDMs display with marked up-regulation of mRNA transcripts for *Nlrp3*, *Il1b*, and *Il18* but neither for *Caspase-1* nor *ASC* (Fig. 4A). Western blot confirmed that protein levels of NLRP3, proIL-1β, and proIL-18 are elevated in *CD1d1*$^{-/-}$ BMDMs (Fig. 4B).

The glycosphingolipid iGb3, normally synthesized by iGb3 synthase (iGb3s), has been proposed to be an endogenous ligand for CD1d1 (*3*). qRT-PCR showed that mouse PEMs and BMDMs have basal levels of *iGb3s* transcripts that can be up-regulated by lipopolysaccharide (LPS) (Fig. 4C). Recognition of LPS by Toll-like receptor 4 (TLR4) recruits intracellular adaptor proteins myeloid differentiation factor 88 (MYD88) and TIR (Toll/interleukin 1 receptor) domain-containing adapter-inducing interferon-β (TRIF) to initiate downstream transcriptional factor signaling for inflammatory gene transcription (*18*). *Myd88*- but not *Trif*- deficiency attenuates LPS-induced *iGb3s* transcription (Fig. 4C). Exogenous iGb3 (5 μg/ml; 12 hours) seemed to inhibit LPS-induced up-regulation of NLRP3, proIL-1β, and proIL-18 proteins in *WT* BMDMs rather than the *CD1d1*$^{-/-}$ counterparts (Fig. 4D). These data suggest that CD1d1 occupancy by iGb3 delivers a negative feedback signal to down-modulate NLRP3, proIL-1β, and proIL-18 mRNA levels in macrophages.

Treating *WT* and *CD1d1*-deficient BMDMs with individual proinflammatory mediators—including nigericin (10 μM; 30 min), adenosine triphosphate (ATP) (5 mM; 30 min), LPS (500 ng/ml; 4 hours), and silica (SiO_2; 10 μM; 45 min)—does not affect caspase-1p20 formation nor IL-1β and IL-18 production (fig. S3), suggesting that *CD1d1* deficiency per se does not cause spontaneous NLRP3 inflammasome activation. However, we found that LPS-primed *CD1d1*$^{-/-}$ BMDMs—when cotreated with ATP, nigericin, or silica—exhibited with more robust induction of NLRP3, caspase-1p20, IL-1βp17, and IL-18p22 expression (Fig. 4E). Therefore, significantly higher levels of IL-1β and IL-18 were also observed in culture supernatants from *CD1d1*$^{-/-}$ BMDMs than *WT* counterparts (Fig. 4F). Conversely, we observed that exposure of iGb3 inhibited caspase-1p20 formation (Fig. 4G) along with consequential IL-1β and IL-18 reduction only in NLRP3 inflammasome-activated *WT* but not *CD1d1*$^{-/-}$ BMDMs (Fig. 4H). iGb3 also blocked the assembly of the NLRP3 inflammasome complex in *WT* BMDMs as visualized via immunofluorescence (Fig. 4I and fig. S4). These results demonstrate that ligation of CD1d1 with iGb3 decreases NLRP3-mediated caspase-1 activation and limits IL-1β/IL-18 secretion from macrophages.

iGb3/CD1d1 inactivates AKT-STAT1-PRDX1–NF-κB signaling in macrophages

NF-κB activation is known to promote the transcription of *Nlrp3*, *Il1b*, and *Il18* (*9*). Using the GenomeNet sequence motif search program (http://motif.genome.jp), we identified multiple binding sites for RelA (also called NF-κBp65) in the *Nlrp3*, *Il1b*, and *Il18* gene promoter regions (fig. S5A), and chromatin immunoprecipitation qPCR (ChIP-qPCR) illustrated that LPS stimulation induced RelA protein binding to the promoter regions of the *Nlrp3*, *Il1b*, and *Il18* genes, while iGB3 administration counteracts these effects (Fig. 5A). We found that iGb3 inhibited LPS-induced inhibitor of nuclear factor κB (IκBα) phosphorylation/degradation and NF-κBp65 phosphorylation in *WT* but not *CD1d1*$^{-/-}$ BMDMs (Fig. 5B). Knockdown of RelA expression in BMDMs by RNA interference (RNAi) attenuated LPS-induced up-regulation of NLRP3, proIL-1β, and proIL-18, both at mRNA and protein levels (Fig. 5C). Similarly, inhibition of IκBα phosphorylation by using the inhibitor BAY11-7082 (25 μM; 12 hours) also prevented LPS-caused NLRP3, proIL-1β, and proIL-18 up-regulation (Fig. 5D), suggesting that classical NF-κB signaling pathway mediates CD1d1/iGb3-dependent inhibition of *Nlrp3*, *Il1b*, and *Il18*.

To further explore the immediate signaling events of iGB3/CD1d1 that lead to NF-κB inactivation, we applied a yeast split-ubiquitin screening system (*13*) using a mouse *CD1d1* C-terminal ubiquitin fusion (pBT3-SUC-*CD1d1*) as the bait against a complementary DNA (cDNA) library constructed from mouse BMDMs (fig. S6A), and we identified 10 candidate CD1d1-interactive genes among 1419 selected clones (fig. S6B). Transient transfection experiments further confirmed that CD1d1 cross-links with all of these identified molecules (fig. S6C). Peroxiredoxin 1 (PRDX1), a protein capable of promoting NF-κB activation via inducing IκBα phosphorylation (*19*), is selected as a contending molecule for transcriptional control of inflammatory genes. Immunofluorescence double staining illustrated that CD1d1 coexpresses with PRDX1 in PEMs (fig. S6D), CD1d1 coimmunoprecipitates PRDX1 protein, and vice versa (fig. S6E). Moreover, iGb3 (5 μg/ml; 12 hours) seemed to cause PRDX1 protein (Fig. 5B) and mRNA (Fig. 5E) reduction only in LPS-primed *WT* but not in *CD1d1*$^{-/-}$ BMDMs. In addition, silencing *Prdx1* expression in BMDMs resulted in attenuation of LPS-induced IκBα and RelA phosphorylation in association with reduced protein expression (Fig. 5F) and mRNA encoding for *RelA*, *Nlrp3*, *Il1b*, and *Il18* (Fig. 5G). The LPS-dependent induction of *Prdx1* mRNA transcription is mediated by AKT/phosphatidylinositol 3-kinase signals (*20*). In agreement, iGb3 significantly reduced phosphorylation of AKT and the downstream signal transducers and activators of transcription 1 (STAT1) in *WT* BMDMs under LPS priming (Fig. 5B). The AKT inhibitor MK2206 (20 μM; 12 hours) efficiently inhibited LPS-induced STAT1 phosphorylation, causing reductions of PRDX1 expression and IκBα phosphorylation, along with down-modulations of NLRP3, proIL-1β, and proIL-18 (Fig. 5H). In addition, the STAT1 inhibitor fludarabine (20 μM; 24 hours) could also inhibit LPS-mediated PRDX1 induction in association with reduction of IκBα and RelA phosphorylation in BMDMs (Fig. 5I). Moreover, we identified multiple binding sites for STAT1 in the *Prdx1* gene promoter regions (fig. S5B), and ChIP-qPCR illustrated that LPS stimulation induced STAT1 protein binding to the promoter regions of *Prdx1* gene, while iGB3 administration reduces this effect (Fig. 5J). These results suggest that iGb3/CD1d1 inactivates NF-κB through inhibition of AKT-STAT1–mediated PRDX1 expression.

The short cytoplasmic tail of CD1d1 contains a tyrosine (Tyr^{332}), which can transmit a positive signal to activate innate immunity (*4*). Mouse RAW264.7 macrophages readily express NLRP3, proIL-1β, and proIL-18 proteins, although lacking caspase-1 inflammasome activity due to the absence of ASC protein (*21*). However, RAW264.7 macrophages can convey a decent transfection efficiency that surpasses primary BMDMs for the examination of the cytoplasmic tail of CD1d1 in signaling transcriptional inhibition of NLRP3 inflammasome components. We generated stable RAW264.7 cells expressing CD1d1 and the CD1d1 variant without the cytoplasmic domain (*CD1d1*$_{\Delta CD}$). iGb3 occupancy of CD1d1 decreases NLRP3, proIL-1β, and proIL-18 in CD1d1^{+}RAW264.7 cells, whereas iGB3 appeared to have no effect on LPS-induced phosphorylation of

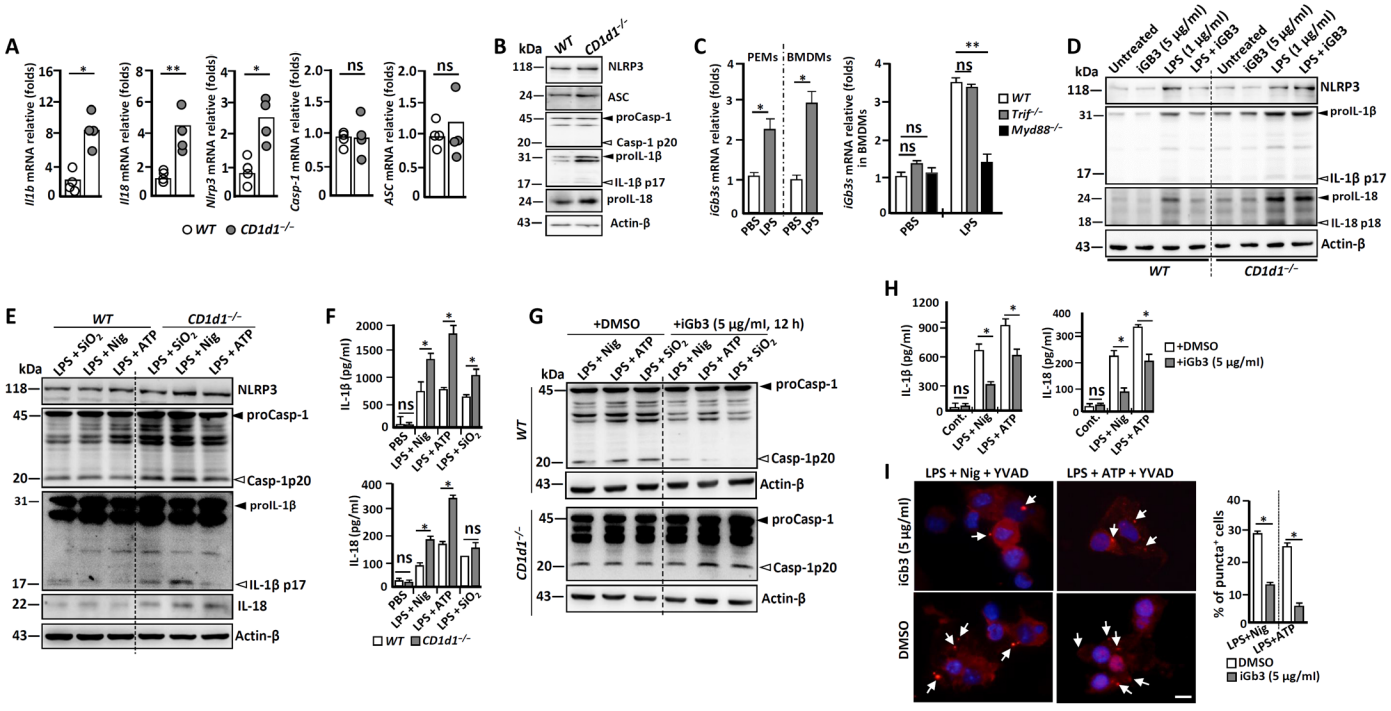

Fig. 4. CD1d1 inhibits the transcription of the *Nlrp3*, *Il1b*, and *Il18* genes in macrophages. BMDMs were collected. (**A**) qRT-PCR analysis of mRNA. (**B**) Immunoblotting analysis of indicated proteins. (**C**) qRT-PCR analysis of *iGb3s* mRNA from indicated BMDMs. (**D**) *WT* and *CD1d1*$^{-/-}$ BMDMs were treated with LPS (1 μg/ml; 6 hours) and iGb3 (5 μg/ml; 12 hours), and cell extracts were immunoblotted for the indicated protein. The NLRP3 inflammasome was activated as described in Materials and Methods, and (**E**) cell extracts were immunoblotted for the indicated proteins. (**F**) ELISA analysis of IL-1β and IL-18 in the culture supernatants. The NLRP3 inflammasome–activated *WT* and *CD1d1*$^{-/-}$ BMDMs were treated with iGb3 (5 μg/ml; 12 hours) or DMSO, and (**G**) cell extracts were immunoblotted for caspase-1p20. (**H**) ELISA analysis of IL-1β and IL-18 in cultured supernatants from *WT* BMDMs. (**I**) The LPS-primed BMDMs were activated by ATP or nigericin (Nig), the caspase-1 inhibitor YVAD was added (20 μM; 30 min) to trap active complexes, cells were fixed and stained for caspase-1 (left), and the percentage of puncta^{+} /total cells were compared (right). Blue indicates nuclear DAPI staining, and arrows indicate positive puncta. Scale bar, 40 μm. More than 100 cells in >10 fields of view in each of three independent experiments were scored. Error bar, SEM. *$P < 0.05$ and **$P < 0.01$; ns, not significantly different (Student's *t* test). Data represent one of three biological replicates, with at least three technical replicates each.

IκBα and RelA in *CD1d1*$_{\Delta CD}$-transfected RAW264.7 cells; thereafter, the up-regulation of NLRP3, proIL-1β, and proIL-18 was unaffected (fig. S7), suggesting that the cytoplasmic tail is essential for CD1d1 intrinsic signal transduction. To further validate the role of Tyr^{332} in iGb3-induced NF-κB inactivation, a RAW264.7 cell line stably expressing a point mutant (Tyr^{332} to Ala^{332}, named *CD1d1*$_{Y332A}$) was established and tested for its response to iGb3 occupancy. *CD1d1*$_{Y332A}$ remains capable of delivering signals to down-modulate phosphorylation of IκBα and RelA, along with reduction in NLRP3, proIL-1β, and proIL-18 expression in these cells (fig. S7). This result suggests that inhibition of NLRP3, proIL-1β, and proIL-18 is independent of Tyr^{332} of CD1d1.

Serine phosphorylation also plays essential roles in protein biological function; we therefore examined a serine (Ser^{330}) in the CD1d1 cytoplasmic tail. We found that LPS induced Ser^{330} phosphorylation (p-Ser) of CD1d1 in *WT* BMDMs, and iGb3 treatment appeared to counteract this effect (Fig. 5K). We therefore created a *CD1d1* point mutant (Ser^{330} to Ala^{330}, named *CD1d1*$_{S330A}$) and established its stable expression in *CD1d1*$^{-/-}$ BMDMs. This *CD1d1* mutant abrogated the iGb3-mediated down-regulation of AKT and STAT1 phosphorylation (Fig. 5L). Collectively, these results reveal that reduction of AKT-STAT1-PRDX1-NF–κB activation and, subsequently, suppression of *Nlrp3*, *Il1b*, and *Il18* transcript expression by iGb3/CD1d1 is via inhibition of CD1d1 Ser^{330} phosphorylation.

Transcription factors JunB and ELK-1 also control *Nlrp3*, *Il1b*, and *Il18* gene expression

In addition to RelA, we identified multiple binding sites for JunB and ETS oncogene-related protein 1 (ELK-1) in the *Nlrp3*, *Il1b*, and *Il18* gene promoter regions based on the GenomeNet sequence motif search program (http://motif.genome.jp) (fig. S5A). Moreover, several RelA-binding sites in *JunB* and *Elk1* gene promoter regions were also identified (fig. S5C), suggesting that RelA-dependent JunB and ELK1 might participate into controlling *Nlrp3*, *Il1b*, and *Il18* transcription.

LPS normally induces JunB and ELK-1 protein expression and phosphorylation in BMDMs in a time-dependent manner (Fig. 6A). Knockdown of *RelA* in BMDMs resulted from reducing LPS-primed *JunB* and *Elk-1* gene transcription (Fig. 6B). Inhibition of NF-κB activity in BMDMs by BAY11-7085 (20 μM; 12 hours) also decreased LPS-induced JunB and ELK-1 phosphorylation (Fig. 6C), indicating the existence of NF-κB–dependent regulation of JunB and ELK-1. In addition, treating *WT* BMDMs with iGb3 resulted in inhibition on the LPS-induced JunB and ELK-1 expression; conversely, iGb3 seemed to exert no effect on the expression of JunB and ELK-1 in *CD1d1*$^{-/-}$ BMDMs (Fig. 6D). In addition, silencing *JunB* (Fig. 6E) and *Elk1* (Fig. 6F) in RAW264.7 cells resulted in a significant reduction of LPS-induced NLRP3, proIL-1β, and proIL-18 gene transcription and protein expressions. ChIP-qPCR illustrated

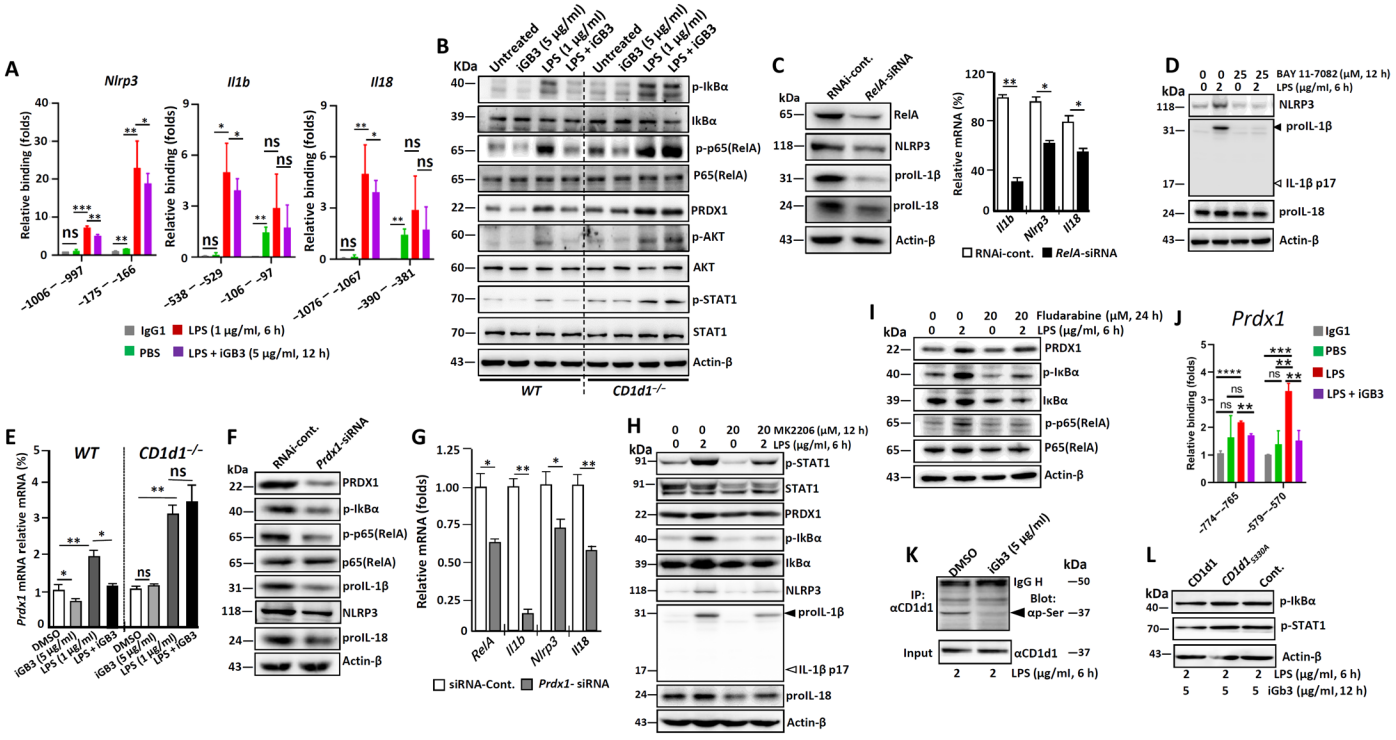

Fig. 5. iGb3/CD1d1 inactivates NF-κB through decreasing PRDX1 expression. Mouse BMDMs were treated with PBS, LPS (1 μg/ml; 6 hours), or LPS and iGb3 (5 μg/ml; 12 hours). (**A**) ChIP-qPCR analysis for RelA protein binding to the promoter regions of indicated genes. *WT* and *CD1d1*$^{-/-}$ BMDMs were treated with LPS (1 μg/ml; 6 hours) or LPS and iGb3 (5 μg/ml; 12 hours), and (**B**) cell extracts were immunoblotted for the indicated molecules. (**C**) The expression of *RelA* in BMDMs was silenced by RNAi; after 48 hours, cells were treated with LPS (1 μg/ml; 6 hours), protein levels were analyzed by immunoblotting (left), and gene transcription was detected by qRT-PCR (right). (**D**) Immunoblotting analysis of indicated protein from BMDMs treated with the NF-κB inhibitor BAY 11-7082. (**E**) Mouse BMDMs were treated with PBS, LPS (1 μg/ml; 6 hours), or LPS and iGb3 (5 μg/ml; 12 hours); qRT-PCR analysis of *Prdx-1* gene transcription. The expression of *Prdx1* in RAW264.7 cells was silenced by RNAi; after 48 hours, cells were further treated with LPS (1 μg/ml; 6 hours). (**F**) Immunoblotting analysis of the indicated proteins. (**G**) qRT-PCR detected gene transcription of the indicated molecules. LPS-primed BMDMs were treated with (**H**) the AKT inhibitor MK2206, (**I**) the STAT1 inhibitor fludarabine; immunoblotting analysis of the indicated molecules. (**J**) Mouse BMDMs were treated with PBS, LPS (1 μg/ml; 6 hours), or LPS and iGb3 (5 μg/ml; 12 hours); ChIP-qPCR analysis for STAT1 protein binding to the promoter regions of *Prdx1* gene. (**K**) CD1d1 immunoprecipitation (IP) from BMDMs and immunoblotting of p-Ser. (**L**) *CD1d1*$^{-/-}$ BMDMs were stably transfected with *CD1d1*-vectors, *CD1d1*$_{S330A}$-vectors or pcDNA3.1(-) vectors (mock), cells were further treated with LPS and iGb3, and cell extracts were immunoblotted for IκBα and STAT1 phosphorylation. Error bar, SEM. *$P < 0.05$ and **$P < 0.01$; ns, not significantly different (Student's *t* test). Data represent one of three biological replicates, with at least three technical replicates each.

that LPS stimulation induced JunB and ELK-1 protein binding to the promoter regions of the *Nlrp3*, *Il1b*, and *Il18* genes from BMDMs, while iGB3 administration counteracts these effects (Fig. 6G). Together, these data indicate that iGB3/CD1d1 initiates the feedback signals leading to transcriptional inhibition of NF-κB itself (RelA) and the NF-κB–dependent JunB and ELK-1 signaling pathways and, therefore, down-modulation of *Nlrp3*, *Il1b*, and *Il18* in macrophages (fig. S8).

DISCUSSION

Activation of NLRP3 inflammasome plays an essential role in mediating the host inflammatory responses against pathogen invasions, and dysregulation of this biological process often causes life-threatening diseases (*10*). Notably, several mechanisms that have been elucidated in the regulation of NLRP3 activities—as well as phosphorylation, adenosine diphosphate–ribosylation, ubiquitination, and nitrosylation—are largely working at posttranscriptional and posttranslational levels (*22*), whereas factors that control the transcription of *Nlrp3* and its immediate substrates such as *Il1b* and *Il18* remain unknown. We here show that CD1d1, a mouse ortholog of human CD1d that mostly expresses on antigen presentation cells for functional presenting lipid-like antigens to NKT cells, is essentially capable of sending intrinsic inhibitory signals for the transcriptional inhibition of *Nlrp3*, *Il1b*, and *Il18* expressions in macrophages. We demonstrated that upon occupancy by glycolipid iGb3, a natural lipid ligand of CD1d1 that seems to be essential for amplification of the innate inflammatory response in monocytes and DCs, it can trigger CD1d1 to send intrinsic negative signals in controlling *Nlrp3* inflammasome expression. Further examination using DSS-induced mouse colitis model reveals that mice with whole genome or macrophage-specific deficiency of *CD1d1* acquire resistance to DSS-caused acute colitis. This protective phenotype attributes to the hyperactivation of NLRP3 inflammasome and consequential elevation of IL-1β and IL-18 secretion during DSS-induced colonic inflammation. Further experiments demonstrate that CD1d1-dependent, macrophage-intrinsic NLRP3 inflammasome activation appears to be critical for stimulating colon epithelial cell proliferation, local IL-10 and IL-22 expression, and T_{reg} infiltration thus to counteract DSS-mediated inflammatory damage. Our data strongly suggest

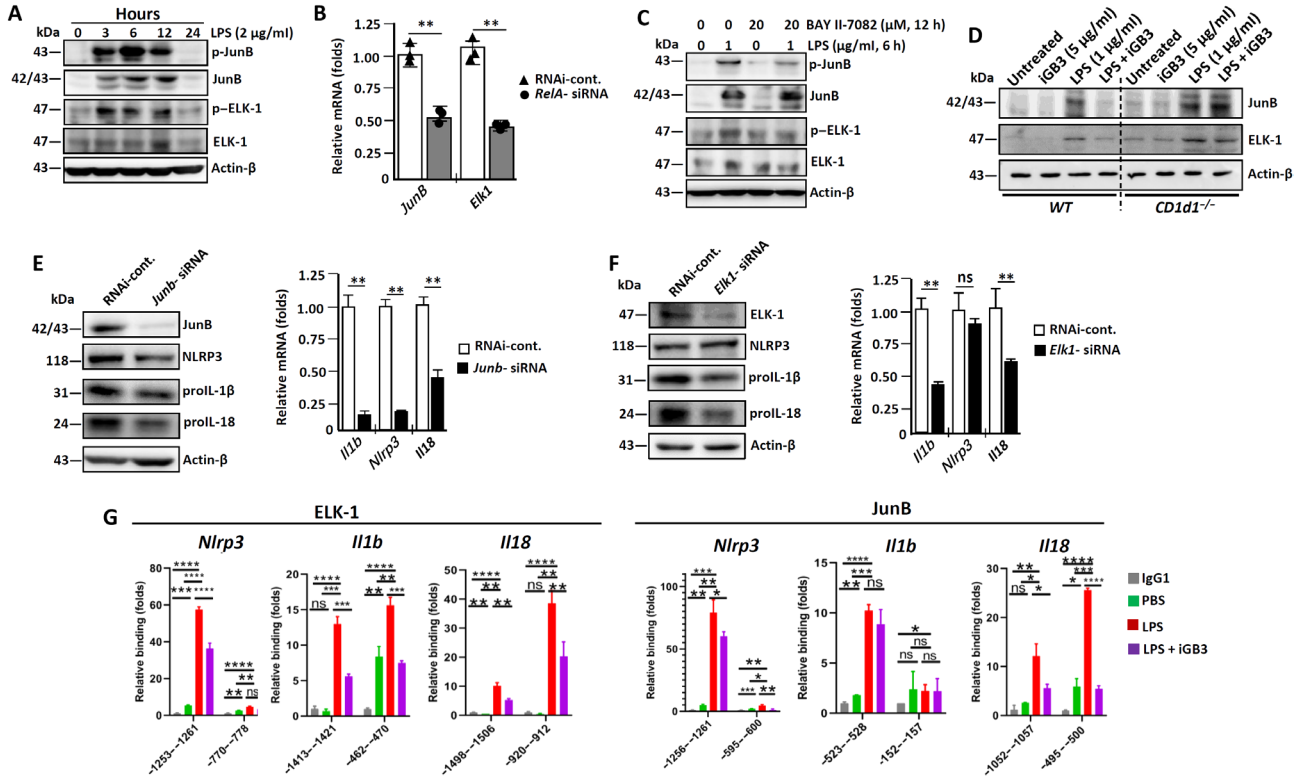

Fig. 6. RelA-dependent JunB and ELK-1 signals exert transcriptional control of *Nlrp3*, *Il1b*, and *Il18* expression. BMDMs were treated with LPS. (**A**) Immunoblotting analysis of the indicated proteins. (**B**) The expression of *RelA* mRNA in BMDMs was silenced by RNAi; after 48 hours, cells were further treated with LPS (1 μg/ml; 6 hours); qRT-PCR analysis of *JunB* and *Elk1* gene expression. (**C**) *WT* and *CD1d1*$^{-/-}$ BMDMs were treated with LPS(1 μg/mL, 6h), iGb3 (5 μg/mL, 12h) or both, cell extracts were immunoblotted for the indicated molecules. (**D**) *WT* and *CD1d1*$^{-/-}$ BMDMs were treated with LPS (1 μg/ml; 6 hours), iGb3 (5 μg/ml; 12 hours) or both, and cell extracts were immunoblotted for the indicated molecules. (**E**) The *JunB* and (**F**) *Elk1* genes in RAW264.7 cells were silenced by RNAi; after 48 hours, cells were further treated with LPS (1 μg/ml; 6 hours); immunoblotting analysis of the induced proteins and qRT-PCR detection of gene transcription. (**G**) ChIP-qPCR analysis for the enrichment of JunB and ELK-1 protein binding to the promoter regions of the indicated genes in *WT* BMDMs. Error bar, SEM; *$P < 0.05$, **$P < 0.01$, ***$P < 0.001$, and ****$P < 0.0001$; ns, no significant difference (Student's *t* test). One of three biological replicates, with three technical replicates.

that CD1d1 mediates intrinsic signals in the suppression of macrophage inflammation and gut epithelial homeostasis thus to reciprocally participate in the pathogenesis of DSS-caused colitis. Therefore, modulating iGb3/CD1d1 signals proposes a therapeutic potential for treating certain NLRP3-associated inflammatory syndromes.

The understanding of *CD1d1* and its roles in IBD pathogenesis has been controversial, debating from the observations of *CD1d*$^{-/-}$ mice having no effect versus that becoming more sensitive toward DSS colitis (*6*, *7*). We here demonstrate that macrophage-specific *CD1d1* deficiency renders mice resistance to DSS-induced colitis (Fig. 3). We show that colonic macrophages are required for the maintenance of intestinal homeostasis during the pathophysiological process of DSS-mediated colitis. Macrophage-associated NLRP3 inflammasome activation, on one hand, results in IL-1β, IL-18, and IL-23 production in favoring local colon tissue inflammation, as evidenced by the observed increase of immune cell infiltration in the gut, and this agrees with the literatures (*23*, *24*). Nevertheless, the NLRP3 inflammasome activation appears to also cause IEC proliferation, IL-10/IL-22 up-regulation, and T_{reg} infiltration, thus to counterbalance DSS-induced tissue damage. Therefore, although there seemed to be more infiltrating immune cells in the affected gut, the overall local tissue damage was less severe in *CD1d1*-deficient mice as evidenced by low leakiness of the intestine-blood barrier compared to *WT* controls. A recent work has showed that *CD1d1* that originated from epitheliums can elicit protective effects in acute colitis by producing more IL-10 (*8*), and CD1d1^{+} B cells also produced IL-10 to decrease chronic intestinal inflammatory condition (*25*). These controversial results suggest broader aspects of tissue distributions of CD1d1 along with diversified biological functions in regulating inflammatory responses in the host. Alterations of the microbiota have a major influence on the outcome of DSS-induced colitis (*26*), and CD1d1 can regulate bacterial colonization in the mouse intestine (*27*). Further studies are needed to clarify whether the observed resistance to DSS-mediated colitis in both *Lym*$^{CD1d1-/-}$ and *CD1d1*$^{-/-}$ mice is also dependent on the altered microbiota in the intestine.

Previous biochemical studies of CD1d1 have focused on its antigen presentation functions for NKT cell activation, with scattered reports claiming that CD1d1 can initiate reciprocal signals to induce secretion of cytokines by both professional and unconventional antigen-presenting cells (APCs) (*4*, *28*). CD1d1 appeared to promote autologous B cell proliferation and Ig production (*29*). Mouse CD1d1 is an MHC-like transmembrane protein with 336 amino acids that has a 10–amino acid cytoplasmic tail. One previous study has shown that the short cytoplasmic tail of CD1d1 contains a putative tyrosine-dependent internalization signal YXXZ (where Y signifies

tyrosine, X is any amino acid, and Z is a hydrophobic amino acid), and Tyr^{332} is responsible for mediating antibody-induced epithelial IL-10 production (*4*). However, our single–amino acid substitution experiments suggest that the iGb3-induced, CD1d1-mediated inhibitory signals for NF-κB activation are Tyr^{332} independent (fig. S7). Instead, we identified that Ser^{330} within the CD1d1 cytoplasmic tail is essential in delivering the inhibitory signals leading to suppression of PRDX1-mediated NF-κB activation (Fig. 5, K and L). Our data illustrate a previously unidentified pathway for immune regulation mediated by CD1d1 in macrophages.

Using a yeast split-ubiquitin screening system, we identified PRDX1 as a protein that associates with CD1d1 (fig. S6). Peroxiredoxins (PRDXs) have been originally described as a family of oxidative stress–inducible peroxidases that comprises with six subtypes (PRDX1~6) in mammalian cells. Together with catalase and glutathione peroxidase, PRDXs involve in the elimination of hydrogen peroxide during oxidative stress–related apoptosis (*19*). Emerging evidence suggests that cellular compartmentalization of PRDX1 can regulate NF-κB activation, and *Prdx1* deficiency seemed to associate with increases in NF-κB–dependent inducible nitric oxide synthase induction and secretion of proinflammatory mediators (*30*). We here showed that iGb3/CD1d1 triggers an inhibitory signal to specifically down-regulate PRDX1 expression in macrophages. In addition to suppress PRDX1 expression, the PRDX1/CD1d1 interactions in the lipid membrane compartments might also reduce free PRDX1 protein in the cytoplasm thus to push on limiting LPS-induced NF-κB activation (*19*). Coming to the proposition of NF-κB signaling in control of the transcription of NLRP3 inflammasome components, we investigated transcriptional factors and found that iGb3/CD1d1 represses RelA and RelA-dependent up-regulation and phosphorylation of JunB and ELK-1 (Fig. 6). RelA and JunB are the key transcriptional activators that induce the transcription of *Tnfα*, *Il6*, and *Il12* genes in BMDCs (bone marrow-derived dendritic cells) through direct promoter binding of these genes. JunB is also required for the LPS-induced full expression of *Il1b* in macrophages. JunB cooperates with interferon regulatory factor 1 (IRF1) and C/EBPβ (a transcription factor, CCAAT/enhancer binding protein β) to facilitate maximal gene expression for *Il6* and *Il12b* in macrophages (*31*). Moreover, two RelA binding sites in the *Nlrp3* gene promoter region have also been described to be responsible for LPS-induced *Nlrp3* transcription (*32*). Here, ChIP-PCR confirmed that RelA directly binds to the promoters of *Nlrp3*, *Il1b*, and *Il18* genes (Fig. 5A). RelA is also an inducer for *JunB* and *Elk1* expression in macrophages, which suggests the existence of NF-κB–dependent signaling cascades, in which NF-κB induces the first wave of the immediate transcriptional factors for the subsequent inductions of proinflammatory cytokine genes that constitute essential steps/checkpoints in macrophage activation.

Although hyperactivation of NLRP3 inflammasome has been shown to deteriorate intestinal inflammatory damage, multiple studies have made opposite observations demonstrating a protective effect of the NLRP3 inflammasome activation on DSS-induced colitis. For examples, $Nlrp3^{-/-}$ and $Casp\text{-}1^{-/-}$ mice developed more severe colitis than *WT* controls due to loss of epithelial integrity and massive leukocyte infiltration (*12*). DSS-fed $Il18^{-/-}$ and $Il18R^{-/-}$ mice have more severe colitis than *WT* controls due to high amounts of interferon-γ and tumor necrosis factor (TNF) (*33*). Moreover, $Il1R1^{-/-}$ mice manifested increased susceptibility to DSS-induced colitis because of reduced expression of IL-10 (*8*). In addition, blocking IL-18 activity by IL-18BP attenuates intestinal damage in DSS-induced colitis (*34*). IL-1β can also induce IL-22 production, which promotes antimicrobial defense, barrier integrity, and tissue repair. Similar to these work, we here show that the $Nlrp3^{-/-}$ and $CD1d1^{-/-}Nlrp3^{-/-}$ DKO mice all manifested with more severe colitis in contrast to *WT* control mice following DSS administration (fig. S1). Moreover, the colonic tissues from DSS-treated $CD1d1^{-/-}$ and $Lym^{CD1d1-/-}$ mice manifested NLRP3 inflammasome hyperactivation, which appears to be critical for stimulating epithelial cell PCNA expression and induces local IL-10 and IL-22 secretion (Figs. 1 and 3). Recently, Yao *et al.* (*35*) showed that IL-1β induces T_{reg} development and inhibits DSS-mediated gut inflammation through inducing adenosine monophosphate production and change microbiota. Zhou *et al.* (*36*) demonstrated that IL-1β can induce IL-2 from group 3 innate lymphoid cells in the gut to promote T_{reg} development, which will harness gut inflammation upon DSS treatment. We here also demonstrated that the colonic tissues from $CD1d1^{-/-}$ mice have a significantly higher percentage of T_{regs} than *WT* littermates after DSS administration thus to counteract DSS-induced inflammatory damage. IL-1Rα is a natural and specific inhibitor of both IL-1β and IL-1α receptor signaling. Bersudsky *et al.* (*37*) reported that IL-1Rα released from damaged IECs acts as an alarmin on initiating and propagating colon inflammation; however, IL-1β is also involved in the IECs' repair and the epithelial barrier reconstitution during resolution of colitis. Using IL-1Rα and IL-18BP, we showed that interruption of IL-1 and IL-18 signaling led to deterioration of DSS colitis in $Lym^{CD1d1-/-}$ mice (fig. S2). In light of the data, we contemplate that interruption of IL-1β/IL-1R1 signaling is responsible for elaboration of DSS-mediated colitis, although aware of the fact that using IL-1Rα would also interrupt IL-1α/IL-1R interactions. In considering with our recent work showing that the resistance of $Vsig4^{-/-}$ mice to DSS-mediated colitis is dependent on the dysregulation of NLRP3/Caspase-1/IL-1β/IL-18 axis (*13*), we postulate that hyperactivation of the NLRP3 inflammasome in gut macrophages can exert a protective effect on acute colitis.

The glycosphingolipid iGb3 has been proposed to be the endogenous ligand essential for thymic invariant NKT cell development, and a variety of lipids has been isolated from biologically occupied CD1d molecules. Although expression of *iGb3s* mRNA has been repeatedly documented in murine tissues including thymus and DCs, the presence of iGb3 in murine macrophages has remained controversial (*38*). We found that BMDMs and PEMs are positive for *iGb3s*, suggesting iGb3 synthesis in macrophages. Recently, Cao's group (*39*) showed that intracellular CD1d1 interacts with PYK2 to promote secretion of proinflammatory cytokines such as TNF and IL-6 from DCs. Nevertheless, we show that iGb3 triggers CD1d1 to down-regulate the transcription of *Nlrp3*, *Il1b*, and *Il18* in macrophages via inactivating the AKT-STAT1-PRDX1–NF-κB cascades. These diverse results may derive from system settings and reagents used in the different experiments. It should be interesting to test CD1d1 signaling pathways using the emerging types of natural CD1d1 binding ligands, such as β-galactosylceramide, sulfatides, disialoganglioside GD3, and phospholipids (*3*).

In summary, our work defines CD1d1 as a negative regulator for transcriptional level control of *Nlrp3* and the inflammasome substrates *Il1b* and *Il18* gene expression. These results shed lights on the development of a novel strategy, for which proper modulation of CD1d1 signaling pathways in combination with other interventions of inflammatory factors might benefit in the treatment of NLRP3-mediated inflammatory diseases in human.

MATERIALS AND METHODS

Mice

The C57BL/6 background *CD1d1*-deficient (*CD1d1*$^{-/-}$, #008881), *CD1d1*$^{fl/fl}$ (#016929), *LyzM-Cre* (#004781), *Nlrp3*$^{-/-}$ (#017970), *Myd88*$^{-/-}$ (#009088), and *WT* mice were purchased from the Jackson laboratory (Bar Harbor, ME, USA). The *Trif*$^{-/-}$ mice on C57BL/6 background were imported from Oriental BioService in Kyoto, Japan. *CD1d1*$^{fl/fl}$ mice were crossed with *LyzM-Cre* mice to develop *Lym*$^{CD1d1-/-}$ mice. Similar methods were used to develop *CD1d1*$^{-/-}$*Nlrp3*$^{-/-}$ DKO mice. All mice were backcrossed 10 times on the B6 background to avoid unpredictable confounders. Mice were maintained in micro-isolator cages, fed with standard laboratory chow diet, and received humane care. All of the experiments were in compliance with the animal study protocol (no. SYXK-PLA-20120031) approved by the Laboratory Animal Welfare and Ethics Committee of the Third Military Medical University (TMMU).

Cells and treatments

Mouse RAW264.7 macrophages were provided by the Cell Institute of the Chinese Academy of Sciences (Shanghai, China). Cells were cultured in six-well plates and propagated in Dulbecco's minimum Eagle's medium supplemented with 10% fetal bovine serum, penicillin (100 U/ml), and streptomycin (100 μg/ml). BMDMs were induced by macrophage colony-stimulating factor as previously described (*13*). In some experiments, cells were treated with the NF-κB inhibitor BAY11-7082 (25 μM; 12 hours; #19542-67-7, Santa Cruz Biotechnology, Dallas, TX, USA), the AKT inhibitor MK220 (20 μM; 12 hours; #SF2712, Beyotime, Shanghai, China), the STAT1 inhibitor fludarabine (20 μM; 24 hours; #sc-204755, Santa Cruz Biotechnology), or iGb3 [dissolved in 0.1% dimethyl sulfoxide (DMSO), 2.5 or 5 μg/ml; Matreya LLC, State College, PA, USA], respectively. LPS (2 μg/ml; #L2630, Sigma-Aldrich, CA, USA) were then added and incubated for an additional 6 hours. To activate NLRP3 inflammasome, BMDMs were first stimulated by LPS (500 ng/ml; 3 hours), cells were further treated with ATP (5 μM; 10 min; #987-65-5, Amresco), nigericin (10 μM; 30 min; #N7143, Sigma-Aldrich), or silica (10 μM; 10 min; #S5130, Sigma-Aldrich), respectively. Cell lysates were generated for Western blot, supernatants were collected, and cytokine release was measured by enzyme-linked immunosorbent assay (ELISA). The IL-1β (#EK0394) and IL-18 (#EK0365) ELISA Kits were purchased from Boster Ltd. (Wuhan, China).

Induction of DSS-mediated acute colitis

Because male *CD1d1*$^{-/-}$ and Lym$^{CD1d1-/-}$ mice are more sensitive to DSS challenge in developing colitis than the female littermates, we therefore only chose to use male mice in this study. Eight-week-old male mice were induced to develop acute colitis by 3.0% (w/v) DSS (molecular weight = 36,000 to 50,000 Da, MP Biomedicals) dissolved in sterile, distilled water ad lib for the experimental days 1 to 6, followed by normal drinking water until the end of the experiment. The DSS solution was made freshly every 2 days. In some experiments, Lym$^{CD1d1-/-}$ mice were intravenously injected with IL-1Rα (2 μg/day per mouse) and IL-18BP (200 ng/day per mouse) 1 day before 3.0% DSS treatment following another 4 days of the same dose of IL-1Rα and IL-18BP. Scoring for stool consistency, occult blood, and measurement of intestinal permeability were done as previously described (*12*). Briefly, a score of 0 indicates well-formed pellets, 1 indicates semi-formed stools that did not adhere to the anus, 2 indicates semi-formed stools that adhered to the anus, and 3 indicates liquid stools that adhered to the anus. Bleeding scores were determined as follows: 0, no blood by using hemoccult; 1, positive hemoccult; 2, blood traces in stool are visible; 3, gross rectal bleeding. Stool consistency scores and bleeding scores were added and presented as clinical score. To analyze epithelial barrier permeability in vivo, food and water were withdrawn at day 6 of the DSS treatment, and these mice were then gavaged with FITC-dextran (60 mg/100 g; molecular weight, 4000; Sigma-Aldrich). Blood was collected after 3 hours, and FITC-dextran amount in serum was measured with a fluorescence spectrophotometer setup with emission and excitation wavelengths of 490 and 520 nm, respectively. In some experiments, strips of colon were mechanically crushed, vortexed in 200 ml of tissue protein extraction reagent (Pierce, Rockford, USA) for 1 min, and shock-frozen in liquid nitrogen. The homogenate was centrifuged at 12,000*g* at 4°C for 20 min, and the amount of IL-1β in the colon homogenate was quantified by ELISA. At the same time, the colon tissues were fixed in 4% formaldehyde, decalcified in EDTA, embedded in paraffin, sectioned, and stained with H&E or used for immunohistochemistry and immunofluorescent staining described later.

Bone marrow chimera

Bone marrow transfer was used to create chimeric mice. Briefly, bone marrows were collected from the femur and tibia of congenic *WT* (expressing CD45.1 leukocyte antigen) or *CD1d1*$^{-/-}$ (expressing CD45.2 leukocyte antigen) donor mice by flushing with Hanks' balanced salt solution. After several washing steps, cells were resuspended at a concentration of 1×10^8/ml. A volume of 100 μl of this cell suspension was retro-orbitally injected in irradiated recipient mice. Four chimera groups were generated: *WT*>*WT* (*WT* cells expressing CD45.1 into *WT* expressing CD45.2), *WT*>*CD1d1*$^{-/-}$ (*WT* cells expressing CD45.1, *CD1d1*$^{-/-}$ expressing CD45.2), *CD1d1*$^{-/-}$> *CD1d1*$^{-/-}$ (*CD1d1*$^{-/-}$ expressing CD45.2 cells into *CD1d1*$^{-/-}$ expressing CD45.2), and *CD1d1*$^{-/-}$>*WT* (*CD1d1*$^{-/-}$ cells expressing CD45.2 into *WT* expressing CD45.1). The use of CD45.1-expressing congenic mice facilitated verification of proper reconstitution in the chimera mice. Bone marrow reconstitution was verified after 5 weeks by staining for CD45.1 and CD45.2 in blood cells using FITC-conjugated anti-CD45.1 and phycoerythrin-conjugated anti-CD45.2. At 7 weeks after bone marrow transfer, mice were fed with 3% DSS for 6 days. Body weight change, stool consistency, and rectal bleeding were monitored daily. At day 7, mice were euthanized, and colon tissues were collected.

Quantitative RT-PCR

The expression of mRNA encoding for indicated genes in BMDMs or RAW264.7 cells were quantified by qRT-PCR with the SYBR Premix ExTaq Kit (Takara). qRT-PCR was performed with specific primers, which are shown in table S1. Results were compared by the $2^{-\Delta\Delta Ct}$ method.

Vector constructs and transduction

The mouse *CD1d1* gene was generated and amplified with a PrimeSTAR PCR mix (Takara, Japan) by using cDNA from mouse BMDMs. The primers are shown in table S1. Purified PCR products were subcloned into the pcDNA3.1(-) vector. On the basis of the mouse *CD1d1* template, a shorter fragment, *CD1d1*$_{\Delta CD}$ (*CD1d1* without the intracellular domain) was further amplified and then inserted

into the pcDNA3.1(-) vector. To obtain the site-directed mutagenesis products of $CD1d1_{Y332A}$ and $CD1d1_{S330A}$, the *CD1d1*- pcDNA3.1(-) vector was mutated using the QuickChange Site-Directed Mutagenesis Kit II (Stratagene, Santa Clara, CA, USA) with special primers (table S1). The RAW264.7 macrophages or BMDMs were transfected with these vectors at a dose of 2 μg per 2×10^6 cells by electroporation following the instructions of Amaxa Nucleofector (4D-Nucleofector, Lonza, Allendale, NJ, USA). The transfection efficiency was assessed by in situ green fluorescent protein expression.

ChIP and qPCR

Both BMDMs and RAW264.7 cells were treated with DMSO, LPS (1 μg/ml; 6 hours), or LPS (1 μg/ml; 6 hours) and iGB3 (5 μg/ml; 12 hours), respectively. Cells were then treated with a SimpleChIP enzymatic ChIP kit [#9003, Cell Signaling Technology (CST)] according to the manufacturers' introductions. Chromatin fragments were prepared by digestion with micrococcal nuclease (0.5 μl per sample; #10011, CST) and sonication. Next, they were labeled with anti-STAT1 (10 μg per sample; #14994, CST), anti-RelA (10 μg per sample; #9182, CST), anti-JunB (10 μg per sample; #3753, CST), and anti–ELK-1 antibodies (10 μg per sample; #9182, CST) or rabbit IgG isotype antibodies (10 μg per sample), respectively. After 24 hours, samples were further incubated with protein G magnetic beads (30 μl per sample; #9006, CST). The chromatin complexes were precipitated in a magnetic separation rack. After that, chromatins were eluted from antibody/protein G magnetic beads and reversed cross-links with protein K (2 μl per sample; #10012, CST). DNA was extracted and purified using spin columns (#10010, CST). qPCR was performed with special primers flanking the putative *Nlrp3*-, *Il1b*-, and *I18*-binding sites, the primers are shown in table S1, and two potential binding sites of each gene were selected. The input DNA was an aliquot of sheared chromatin before immunoprecipitation and was used for normalization of the samples to the amount of chromatin added to each ChIP.

siRNA transfection in vitro

Small interfering RNA (siRNA) was introduced into BMDMs or RAW264.7 by electroporation in a concentration of 20 nM (Amaxa Nucleofector, Lonza). The RNAi targeting sequences of the indicated molecules are shown in table S1. The negative control siRNA (medGCduplex #2 and #3) was purchased from Invitrogen. After 48 hours of transfection, cells were replaced with fresh medium. In some experiments, cells were further treated with LPS (2 μg/ml; 6 hours). The expression of the indicated molecules was detected by qRT-PCR and Western blots, respectively.

Split-ubiquitin screening with macrophage libraries

For screening potential interactive protein partners, the pBT3-SUC vector supplied by the manufacturer (Dualsystems Biotech) was used as a bait vector. The *CD1d1* encoding sequence were obtained from *CD1d1*-pcDNA3.1(-) plasmids and cloned into pBT3-SUC vector. The primers are as follows: pBT3-SUC-F (5′-TGGCATG-CATGTGCTCTG-3′) and pPR3-N-F (5′-GTCGAAAATTCAAG-ACAAGG-3′). The macrophage cDNA libraries in the prey vector pPR3-N were used for yeast two-hybrid screening. cDNA libraries were constructed according to the manual for the split-ubiquitin system (Dualsystems Biotech). The bait constructs were transfected into the yeast reporter strain NMY51 via standard procedures. For screening, the library plasmids were introduced into the yeast cells harboring bait constructs. After 3 days, transformants were grown under selective medium lacking leucine, tryptophan, histidine, and adenine, with the addition of 20 mM 3-amino-1,2,4-triazole. Library plasmids were isolated from positive clones and retransformed into NMY51 to test bait dependency. Only preys that activated the histidine and adenine reporters in the presence of *CD1d1* but not pBT3-SUC were considered true interactors. Last, 10 positive clones were isolated from 1419 clones of the first-round library screening.

Immunofluorescence

To detect CD1d1 and PRDX1 colocalization, PEMs were stained with anti-CD1d1 (1:100; #123504, BioLegend) and anti-PRDX1 (1:100; #ab41906, Abcam) antibodies at 4°C overnight, and cells were then stained with Alexa Fluor 488–conjugated (#A-21206, Thermo Fisher Scientific, Billerica, MA, USA) and Alexa Fluor 555–conjugated (#A-21422, Thermo Fisher Scientific) secondary antibodies for 1 hour. To detect NLRP3 puncta in BMDMs, YVAD (40 μM; BioVision) were added following LPS priming, 30 min before the addition of the NLRP3 inflammasome activators as described previously (*40*). Cells were then stained with anti–Caspase-1 (1:100; AG-20B-0042, AdipoGen) antibodies overnight at 4°C. Sections were added with DAPI (4′,6-diamidino-2-phenylindole) for incubation for 10 min. Sections were washed with PBS, mounted, and analyzed using fluorescence microscopy (Zeiss Axioplan 2).

Western blots

Protein expression was detected by Western blots in macrophages or colon tissues. Briefly, cells or tissues were lysed using radioimmunoprecipitation assay lysis buffer [#P0013B, Beyotime, Shanghai, China; 50 mM tris (pH 7.4), 150 mM NaCl, 1% Triton X-100, 1% sodium deoxycholate, 0.1% SDS, 10 mM EDTA (pH 8.0), leupeptin (5 μg/ml), and 1 mM phenylmethylsulfonyl fluoride]. The cell lysates were centrifuged, and the supernatants were mixed with the same amount of SDS sample buffer. After boiling, samples were separated through electrophoresis and transferred to polyvinylidene difluoride membranes. The membranes were probed with the appropriate antibodies and detected using a Kodak Digital Image Station 4000MM system (Eastman Kodak). The following antibodies were used: anti–actin-β (#3700, CST), anti-CD1d1 (#123504, BioLegend), anti-PRDX1 (#ab41906, Abcam), anti-STAT1 (#9177, CST), anti-p-STAT1 (#9172, CST), anti-PCNA (#13100, CST), anti-JunB (#3753, CST), anti-HSP90 (#4875, CST), anti-p-JunB (#8053, p-Thr^{102}/p-Thr^{104}, CST), anti–ELK-1 (#9182, CST), anti-p-ELK-1 (#9182, p-Ser^{383}, CST), anti-p-IκBα (#2859, p-Ser^{32}, CST), anti-IκBα (#4812, CST), anti-AKT (#2920, CST), anti–p-AKT (p-Thy^{308}, #4056; p-Ser^{473}, #4051, CST), anti–p-p65 (#3033, CST), anti-ASC (#sc-376916, Santa Cruz Biotechnology), anti–IL-18 (#ab71495, Abcam), anti–IL-18 (#AB71495, Abcam, Cambridge, MA, USA), anti–IL-22 (#ab18564, Abcam), anti–IL-10 (#sc-365858, Santa Cruz Biotechnology), anti–IL-1β (#ab9722, Abcam), anti–caspase-1 (#AG-20B-0042, AdipoGen, San Diego, CA, USA), and anti-NLRP3 (#AG-20B-0014-C100, AdipoGen). The dilution of primary antibodies was 1:1000 to 1:5000.

Flow cytometry

To detect CD1d1 on the surface of immune cells, leukocytes from mouse blood were collected. On the other hand, the colonic tissues from indicated mice were isolated and were liberated by digestion with Liberase C (1.6 U/ml; Roche) and deoxyribonuclease I (0.2 mg/ml; Roche) for 2 hours at room temperature. The dead cells were excluded

first by staining with the LIVE/DEAD Fixable Near-Infrared Dead Cell Stain Kit (Life Technologies, Eugene, OR, USA). To measure the expression of phenotype markers on the cell surface, suspended cells were incubated for 1 hour at room temperature in the dark using fluorescent antibodies (anti-CD11c, anti-B220, anti-NK1.1, anti-CD4, anti-CD8, anti-CD45, anti-Foxp3, anti-Ly6G, anti-Ly6C, and anti-F4/80; eBioscience, San Diego, CA, USA). A total of 10,000 live cells were analyzed by FACsAria cytometer (BD, Franklin Lakes, NJ, USA). The gate strategy is shown in fig. S9. All flow cytometry data were analyzed using CellQuest Pro software.

Statistical analysis

Survival data from in vivo experiments were analyzed by a log-rank test performed on curves generated by GraphPad Prism 7.0 (Software MacKiev). For all other analysis, two-tailed, unpaired Student's *t* tests with a 95% confidence interval performed on graphs generated in GraphPad Prism were used. Error bars represent the SEM. $P < 0.05$ was considered as a statistically significant difference. All results shown are representative of at least three separate experiments.

SUPPLEMENTARY MATERIALS

Supplementary material for this article is available at http://advances.sciencemag.org/cgi/content/full/6/43/eaaz7290/DC1

View/request a protocol for this paper from *Bio-protocol*.

REFERENCES AND NOTES

1. G. E. Fragoulis, C. Liava, D. Daoussis, E. Akriviadis, A. Garyfallos, T. Dimitroulas, Inflammatory bowel diseases and spondyloarthropathies: From pathogenesis to treatment. *World J. Gastroenterol.* **25**, 2162–2176 (2019).
2. I. Okayasu, S. Hatakeyama, M. Yamada, T. Ohkusa, Y. Inagaki, R. Nakaya, A novel method in the induction of reliable experimental acute and chronic ulcerative colitis in mice. *Gastroenterology* **98**, 694–702 (1990).
3. R. M. McEwen-Smith, M. Salio, V. Cerundolo, CD1d-dependent endogenous and exogenous lipid antigen presentation. *Curr. Opin. Immunol.* **34**, 116–125 (2015).
4. S. P. Colgan, R. M. Hershberg, G. T. Furuta, R. S. Blumberg, Ligation of intestinal epithelial CD1d induces bioactive IL-10: Critical role of the cytoplasmic tail in autocrine signaling. *Proc. Natl. Acad. Sci. U.S.A.* **96**, 13938–13943 (1999).
5. L. J. Saubermann, P. Beck, Y. P. De Jong, R. S. Pitman, M. S. Ryan, H. S. Kim, M. Exley, S. Snapper, S. P. Balk, S. J. Hagen, O. Kanauchi, K. Motoki, T. Sakai, C. Terhorst, Y. Koezuka, D. K. Podolsky, R. S. Blumberg, Activation of natural killer T cells by alpha-galactosylceramide in the presence of CD1d provides protection against colitis in mice. *Gastroenterology* **119**, 119–128 (2000).
6. H. S. Kim, D. H. Chung, IL-9-producing invariant NKT cells protect against DSS-induced colitis in an IL-4-dependent manner. *Mucosal Immunol.* **6**, 347–357 (2013).
7. T. Selvanantham, Q. Lin, C. X. Guo, A. Surendra, S. Fieve, N. K. Escalante, D. S. Guttman, C. J. Streutker, S. J. Robertson, D. J. Philpott, T. Mallevaey, NKT cell-deficient mice harbor an altered microbiota that fuels intestinal inflammation during chemically induced colitis. *J. Immunol.* **197**, 4464–4472 (2016).
8. T. Olszak, J. F. Neves, C. M. Dowds, K. Baker, J. Glickman, N. O. Davidson, C.-S. Lin, C. Jobin, S. Brand, K. Sotlar, K. Wada, K. Katayama, A. Nakajima, H. Mizuguchi, K. Kawasaki, K. Nagata, W. Müller, S. B. Snapper, S. Schreiber, A. Kaser, S. Zeissig, R. S. Blumberg, Protective mucosal immunity mediated by epithelial CD1d and IL-10. *Nature* **509**, 497–502 (2014).
9. P. Broz, V. M. Dixit, Inflammasomes: Mechanism of assembly, regulation and signalling. *Nat. Rev. Immunol.* **16**, 407–420 (2016).
10. T. Strowig, J. Henao-Mejia, E. Elinav, R. Flavell, Inflammasomes in health and disease. *Nature* **481**, 278–286 (2012).
11. A.-C. Villani, M. Lemire, G. Fortin, E. Louis, M. S. Silverberg, C. Collette, N. Baba, C. Libioulle, J. Belaiche, A. Bitton, D. Gaudet, A. Cohen, D. Langelier, P. R. Fortin, J. E. Wither, M. Sarfati, P. Rutgeerts, J. D. Rioux, S. Vermeire, T. J. Hudson, D. Franchimont, Common variants in the *NLRP3* region contribute to Crohn's disease susceptibility. *Nat. Genet.* **41**, 71–76 (2009).
12. M. H. Zaki, K. L. Boyd, P. Vogel, M. B. Kastan, M. Lamkanfi, T.-D. Kanneganti, The NLRP3 inflammasome protects against loss of epithelial integrity and mortality during experimental colitis. *Immunity* **32**, 379–391 (2010).
13. X. Huang, Z. Feng, Y. Jiang, J. Li, Q. Xiang, S. Guo, C. Yang, L. Fei, G. Guo, L. Zheng, Y. Wu, Y. Chen, VSIG4 mediates transcriptional inhibition of *Nlrp3* and *Il-1β* in macrophages. *Sci. Adv.* **5**, eaau7426 (2019).
14. J. L. Bishop, M. E. Roberts, J. L. Beer, M. Huang, M. K. Chehal, X. Fan, L. A. Fouser, H. L. Ma, J. T. Bacani, K. W. Harder, Lyn activity protects mice from DSS colitis and regulates the production of IL-22 from innate lymphoid cells. *Mucosal Immunol.* **7**, 405–416 (2014).
15. K. Sugimoto, A. Ogawa, E. Mizoguchi, Y. Shimomura, A. Andoh, A. K. Bhan, R. S. Blumberg, R. J. Xavier, A. Mizoguchi, IL-22 ameliorates intestinal inflammation in a mouse model of ulcerative colitis. *J. Clin. Invest.* **118**, 534–544 (2008).
16. M. Nakayama, Macrophage Recognition of Crystals and Nanoparticles. *Front. Immunol.* **9**, 103 (2018).
17. W. P. Arend, G. Palmer, C. Gabay, IL-1, IL-18, and IL-33 families of cytokines. *Immunol. Rev.* **223**, 20–38 (2008).
18. L. A. J. O'Neill, D. Golenbock, A. G. Bowie, The history of Toll-like receptors - redefining innate immunity. *Nat. Rev. Immunol.* **13**, 453–460 (2013).
19. J. M. Hansen, S. Moriarty-Craige, D. P. Jones, Nuclear and cytoplasmic peroxiredoxin-1 differentially regulate NF-κB activities. *Free Radic. Biol. Med.* **43**, 282–288 (2007).
20. A. Bast, K. Fischer, S. F. Erttmann, R. Walther, Induction of peroxiredoxin I gene expression by LPS involves the Src/PI3K/JNK signalling pathway. *Biochim. Biophys. Acta* **1799**, 402–410 (2010).
21. P. Pelegrin, C. Barroso-Gutierrez, A. Surprenant, P2X7 receptor differentially couples to distinct release pathways for IL-1beta in mouse macrophage. *J. Immunol.* **180**, 7147–7157 (2008).
22. J. Yang, Z. Liu, T. S. Xiao, Post-translational regulation of inflammasomes. *Cell. Mol. Immunol.* **14**, 65–79 (2017).
23. J.-E. Ghia, F. Galeazzi, D. C. Ford, C. M. Hogaboam, B. A. Vallance, S. Collins, Role of M-CSF-dependent macrophages in colitis is driven by the nature of the inflammatory stimulus. *Am. J. Physiol. Gastrointest. Liver Physiol.* **294**, G770–G777 (2008).
24. J. E. Qualls, A. M. Kaplan, N. van Rooijen, D. A. Cohen, Suppression of experimental colitis by intestinal mononuclear phagocytes. *J. Leukoc. Biol.* **80**, 802–815 (2006).
25. A. Mizoguchi, E. Mizoguchi, H. Takedatsu, R. S. Blumberg, A. K. Bhan, Chronic intestinal inflammatory condition generates IL-10-producing regulatory B cell subset characterized by CD1d upregulation. *Immunity* **16**, 219–230 (2002).
26. A. R. Weingarden, B. P. Vaughn, Intestinal microbiota, fecal microbiota transplantation, and inflammatory bowel disease. *Gut Microbes* **8**, 238–252 (2017).
27. E. E. S. Nieuwenhuis, T. Matsumoto, D. Lindenbergh, R. Willemsen, A. Kaser, Y. Simons-Oosterhuis, S. Brugman, K. Yamaguchi, H. Ishikawa, Y. Aiba, Y. Koga, J. N. Samsom, K. Oshima, M. Kikuchi, J. C. Escher, M. Hattori, A. B. Onderdonk, R. S. Blumberg, Cd1d-dependent regulation of bacterial colonization in the intestine of mice. *J. Clin. Invest.* **119**, 1241–1250 (2009).
28. S. C. Yue, M. Nowak, A. Shaulov-Kask, R. J. Wang, D. Yue, S. P. Balk, M. A. Exley, Direct CD1d-mediated stimulation of APC IL-12 production and protective immune response to virus infection in vivo. *J. Immunol.* **184**, 268–276 (2010).
29. S.-J. Kang, P. Cresswell, Regulation of intracellular trafficking of human CD1d by association with MHC class II molecules. *EMBO J.* **21**, 1650–1660 (2002).
30. S.-U. Kim, Y.-H. Park, J.-S. Min, H.-N. Sun, Y.-H. Han, J.-M. Hua, T.-H. Lee, S.-R. Lee, K.-T. Chang, S. W. Kang, J.-M. Kim, D.-Y. Yu, S.-H. Lee, D.-S. Lee, Peroxiredoxin I is a ROS/p38 MAPK-dependent inducible antioxidant that regulates NF-κB-mediated iNOS induction and microglial activation. *J. Neuroimmunol.* **259**, 26–36 (2013).
31. Q. Liu, Y. Zhu, W. K. Yong, N. S. K. Sze, N. S. Tan, J. L. Ding, Cutting Edge: Synchronization of IRF1, JunB, and C/EBPβ Activities during TLR3-TLR7 Cross-Talk Orchestrates Timely Cytokine Synergy in the Proinflammatory Response. *J. Immunol.* **195**, 801–805 (2015).
32. F. G. Bauernfeind, G. Horvath, A. Stutz, E. S. Alnemri, K. M. Donald, D. Speert, T. Fernandes-Alnemri, J. Wu, B. G. Monks, K. A. Fitzgerald, V. Hornung, E. Latz, Cutting edge: NF-κB activating pattern recognition and cytokine receptors license NLRP3 inflammasome activation by regulating NLRP3 expression. *J. Immunol.* **183**, 787–791 (2009).
33. H. Takagi, T. Kanai, A. Okazawa, Y. Kishi, T. Sato, H. Takaishi, N. Inoue, H. Ogata, Y. Iwao, K. Hoshino, K. Takeda, S. Akira, M. Watanabe, H. Ishii, T. Hibi, Contrasting action of IL-12 and IL-18 in the development of dextran sodium sulphate colitis in mice. *Scand. J. Gastroenterol.* **38**, 837–844 (2003).
34. P. V. Sivakumar, G. M. Westrich, S. Kanaly, K. Garka, T. L. Born, J. M. J. Derry, J. L. Viney, Interleukin 18 is a primary mediator of the inflammation associated with dextran sulphate sodium induced colitis: Blocking interleukin 18 attenuates intestinal damage. *Gut* **50**, 812–820 (2002).
35. X. Yao, C. Zhang, Y. Xing, G. Xue, Q. Zhang, F. Pan, G. Wu, Y. Hu, Q. Guo, A. Lu, X. Zhang, R. Zhou, Z. Tian, B. Zeng, H. Wei, W. Strober, L. Zhao, G. Meng, Remodelling of the gut microbiota by hyperactive NLRP3 induces regulatory T cells to maintain homeostasis. *Nat. Commun.* **8**, 1896 (2017).
36. L. Zhou, C. Chu, F. Teng, N. J. Bessman, J. Goc, E. K. Santosa, G. G. Putzel, H. Kabata, J. R. Kelsen, R. N. Baldassano, M. A. Shah, R. E. Sockolow, E. Vivier, G. Eberl, K. A. Smith, G. F. Sonnenberg, Innate lymphoid cells support regulatory T cells in the intestine through interleukin-2. *Nature* **568**, 405–409 (2019).
37. M. Bersudsky, L. Luski, D. Fishman, R. M. White, N. Ziv-Sokolovskaya, S. Dotan, P. Rider, I. Kaplanov, T. Aychek, C. A. Dinarello, R. N. Apte, E. Voronov, Non-redundant properties of IL-1α and IL-1β during acute colon inflammation in mice. *Gut* **63**, 598–609 (2014).

38. J. Milland, D. Christiansen, B. D. Lazarus, S. G. Taylor, P. X. Xing, M. S. Sandrin, The molecular basis for galalpha(1,3)gal expression in animals with a deletion of the α1,3galactosyltransferase gene. *J. Immunol.* **176**, 2448–2454 (2006).
39. X. Liu, P. Zhang, Y. Zhang, Z. Wang, S. Xu, Y. Li, W. Huai, Q. Zhou, X. Chen, X. Chen, N. Li, P. Wang, Y. Li, X. Cao, Glycolipid iGb3 feedback amplifies innate immune responses via CD1d reverse signaling. *Cell Res.* **29**, 42–53 (2019).
40. T. Murakami, J. Ockinger, J. Yu, V. Byles, A. M. Coll, A. M. Hofer, T. Horng, Critical role for calcium mobilization in activation of the NLRP3 inflammasome. *Proc. Natl. Acad. Sci. U.S.A.* **109**, 11282–11287 (2012).

Acknowledgments
Funding: This work was supported by The National Key Research and Development Program of China (2016YFA0502204) and the National Natural Science Foundation of China (NSFC; nos. 81971478, 81771691, 81701551, and 81361120400). L.Z. is supported by the Intramural Research Programs, Laboratory of Immune System Biology, National Institute of Allergy and Infectious Diseases, NIH, USA. **Author contributions:** L.Z. and Y.C. were involved in the final development of the project and manuscript preparation. Y.C., Q.Z., J.H., and Y.W. analyzed the data. S.C., X.H., J.L., Z.F., W.B., Y.P., and C.W. performed most of the experiments including Western blot and ELISA. Q.X., L.F., and H.Y. conducted the plasmid mutation. Y.C. and S.C. did flow cytometry analysis. **Competing interests:** The authors declare that they have no competing interests. **Data and materials availability:** All data needed to evaluate the conclusions in the paper are present in the paper and/or the Supplementary Materials. Additional data related to this paper may be requested from the authors.

Submitted 3 October 2019
Accepted 8 September 2020
Published 21 October 2020
10.1126/sciadv.aaz7290

Citation: S. Cui, C. Wang, W. Bai, J. Li, Y. Pan, X. Huang, H. Yang, Z. Feng, Q. Xiang, L. Fei, L. Zheng, J. Huang, Q. Zhang, Y. Wu, Y. Chen, CD1d1 intrinsic signaling in macrophages controls NLRP3 inflammasome expression during inflammation. *Sci. Adv.* **6**, eaaz7290 (2020).